Modifying metal–polymer nanostructures using UV exposure

Nataliya Yufa,[a] Stephanie Fronk,[b] Seth B. Darling,[c] Ralu Divan,[c] W. Lopes[d] and S. J. Sibener*[b]

Received 20th November 2008, Accepted 23rd January 2009
First published as an Advance Article on the web 2nd March 2009
DOI: 10.1039/b820775e

Metals have a variety of behaviors when deposited onto diblock copolymer films, in particular, poly(styrene-*b*-methylmethacrylate). Silver is known to form nanowires, whereas gold forms ellipsoidal nanoparticles of different sizes on each of the blocks, and chromium creates a uniform film on PS-*b*-PMMA. We show that with UV light we can alter the separation between silver nanowires, by making each wire narrower. We also demonstrate the effects of UV light on PS-*b*-PMMA coated with thin layers of gold and chromium, as observed with atomic force microscopy and transmission electron microscopy. We have found that UV exposure increased corrugation of such metal–polymer hybrids by removing PMMA domains, but did not remove metal residing on top of those domains. The ability to manipulate the morphology of these nanomaterials has potential application in areas such as electronics and sensor technology.

Introduction

Diblock copolymers are polymer chains consisting of two chemically distinct blocks, connected by a covalent bond. Microphase separation into a variety of nanoscale structures makes them an attractive template for a variety of applications, including nanoscale lithography, organic–inorganic hybrid materials, electronics, and magnetic memory.[1–13] One commonly studied diblock copolymer is poly(styrene-*block*-methylmethacrylate) (PS-*b*-PMMA), which is valued for having both blocks present at the surface in thin films.[14–16] This copolymer has been used to make ordered arrays,[11,17,18] as a lithographic template,[19] and as a scaffold for colloidal nanoparticles[19–24] and proteins.[25] The two blocks of PS-*b*-PMMA are chemically and physically distinct, which makes many of these applications possible. For example, lithography and in some cases scaffolding rely on the different etching rates of PS and PMMA when exposed to reactive ion etching or UV light.

We and others have shown previously that UV exposure can remove PMMA, while cross-linking the PS.[20,22] This suggests a possible route to the creation and modification of hybrid metal–polymer surfaces by depositing the metals first, then exposing the sample to deep UV light to remove PMMA.

There are several techniques for depositing metals to create nanostructures, such as thermal deposition and chemical vapor deposition.[26,27] Resulting structures may differ depending on the technique. Thermal metal deposition consists of heating a boat with metal to cause metal to evaporate and coat the sample. Using thermal deposition, Lopes and Jaeger have shown that selected metals coat certain blocks within this diblock copolymer preferentially, due to different rates of diffusion and surface energies of metal on each block.[26] However, with thermal metal deposition, selective decoration occurred only with repeated metal deposition followed by annealing for most metals, with the exception of silver which formed nanowires after a single coating.[26] Sputter-coating is a different metal-deposition technique, where plasma is used to eject particles from the target metal which then coat the sample. Although the metal itself is not heated, it is possible that the delicate PS-*b*-PMMA films are damaged as a result of the coating process. We have prepared samples coated with chromium and titanium using sputter-coating, and found that their corrugation was unchanged following exposure to UV light. This suggests that PMMA may have been etched away during the sputtering process. However, a recent unpublished study by S. Darling using gold showed that sputter-coating may lead to selective adsorption without resorting to annealing.

Gold and silver display higher coverage on PS, while tin, bismuth, and lead selectively decorate the PMMA.[28] Exposure to high-energy irradiation, such as an accelerated electron beam in a scanning electron microscope, can significantly affect the surface diffusion behavior of metals on block copolymer films.[29]

An additional degree of freedom in creating metal–organic hybrids can extend the structures' usefulness. For example, a structure having metal nanowires and nanoscale corrugation can be used simultaneously for its conducting properties and as a scaffold for magnetic nanoparticles.

Experimental

Syndiotactic diblock PS-*b*-PMMA (77 000 g/mol, 70% PS) was obtained from Polymer Source, Inc. Thin films were spin-coated from ~1.5% toluene solution onto ultrasonically cleaned silicon nitride substrates, at 3000–6000 rpm. The resulting films were 25–35 nm thick on average—approximately a monolayer of PMMA cylinders in a matrix of PS, with a horizontal period spacing of 40 nm and cylinder diameter of 20 nm—as determined by a combination of AFM and optical measurements. The samples were heated to 518 K in an argon atmosphere at a rate of

[a]*James Frank Institute and Department of Physics, The University of Chicago, Chicago, IL 60637, USA*
[b]*James Franck Institute and Department of Chemistry, The University of Chicago, Chicago, IL 60637, USA. E-mail: s-sibener@uchicago.edu*
[c]*Center for Nanoscale Materials, Argonne National Laboratory, Argonne, IL 60439, USA*
[d]*Department of Physics, Williams College, Williamstown, MA 01267, USA*

5 K/min, and kept at that temperature for between 5 min and 12 h, then cooled to room temperature at 1–2 K/min. The films were first coated with metal and then irradiated with UV light. For UV exposure, the samples were placed 10 inches away from a deuterium Hamamatsu L2793 lamp in rough vacuum of 10–100 mTorr, with a measured flux of 600 $\mu W/cm^2$, and exposed to the light for 15 min. Additional exposure did not cause further increase in corrugation.

Metal coating was performed thermally to deposit silver, chromium or gold, at rates of 0.5–1 Å/s. The nominal thicknesses of the metal layers were measured by a quartz crystal microbalance and were between 0.1 and 12 nm. Since most of the metals do not coat PS-*b*-PMMA uniformly, actual local thicknesses varied. The samples were imaged using tapping mode on a Veeco Multimode IV AFM to observe their topography. Using TEM window substrates ($20 \times 20\ \mu m^2$ silicon nitride membrane fabricated using a silicon micromachining technique),[30] samples were also imaged using a FEI 30 transmission electron microscope (TEM) at 100 and 300 keV. *Image J* processing software, obtained from NIH, was used to analyze TEM data.[31]

Results

Silver

Lopes[28] has found that without additional heating during or after metal evaporation, silver forms nanowires (seen as dark shades of gray) on top of PS domains in PS-*b*-PMMA films, as shown in Fig. 1a. This is due to a combination of silver having a slower mobility on PS than PMMA, as well as a lower surface tension with PS than with PMMA.[32] The contrast due to silver is not identical everywhere. Previously, this has been attributed to different crystal lattice orientations within the silver domains.[28]

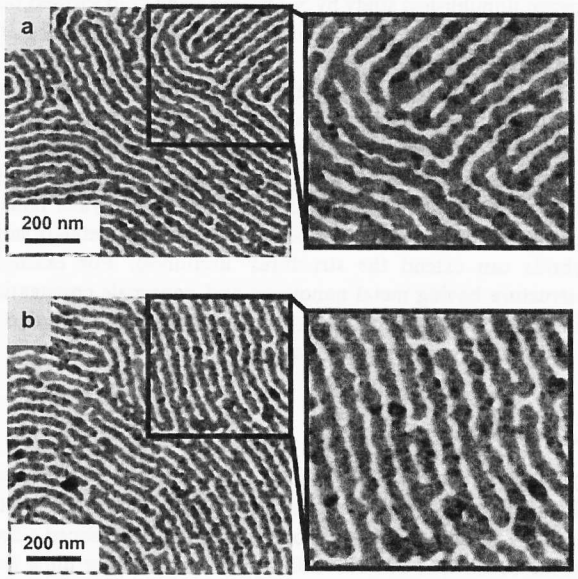

Fig. 1 TEM images of silver nanowires formed by depositing 12 nm of silver onto pristine PS-*b*-PMMA films: (a) before UV irradiation, (b) after UV irradiation. The average separation between domains increased by 20 percent following irradiation. This means that silver wires narrowed, but are still wider than the original PS domains.

Another possibility is silver thickness variation, which has been observed in AFM images (not shown). A nominal thickness of approximately 12 nm is necessary to make the wires continuous, while deposition rates can be as high as 5 Å/s. As TEM data show, silver rests primarily, but not exclusively, on top of the PS domains. From TEM micrographs we know that the width of the silver wires is 35 nm on average, while the PS domains are only 20 nm wide, which means silver spills over onto PMMA domains. This phenomenon is potentially detrimental to future applications because neighboring wires could connect with each other electrically.

Fig. 1b shows the result of UV exposure on the silver nanowire–diblock hybrid, as viewed by TEM. Wire narrowing occurs because UV light selectively removes PMMA (including the silver residing on top of it), and in the process increases the separation between silver wires on average by 20 percent. This figure was determined as follows: the total area of the region between silver wires in two typical TEM images of $1 \times 1\ \mu m^2$ was measured using *Image J* to go from 31 to 37 percent following UV exposure. Since the length of the silver wires was unchanged, the separation between the silver increased by approximately 20 percent.

While the exact mechanism for this has not yet been elucidated, we do know that the wires are not becoming smoother. The increase in nanowire spacing can be an advantage for certain electronic applications, where close contact between wires needs to be avoided to minimize the potential for short circuiting between adjacent wires.

Chromium

We coated diblock copolymer thin films with 1–2.5 nm of chromium, deposited at a slow rate of 0.1 Å/s or less to prevent metal aggregation. Without UV exposure, the corrugation usually seen in films of this polymer was greatly reduced as observed with AFM (Fig. 2a). Following UV illumination, the corrugation increased beyond the typical sub-nanometre levels of a pristine diblock film, suggesting PMMA removal, as shown in Fig. 2c. The corrugation varied between 5 and 10 nm. TEM images, which "look through" the sample and not just the surface, did not show any evidence of chromium stripes located on PS domains, as might be expected if the previously uniform film were patterned by lift-off from the PMMA domains. The fact that corrugation increased, while no clear metal stripes formed, suggests that a more corrugated, uniformly chromium-coated surface was created. This increased corrugation without clear stripes of metal is similar to our findings for gold discussed below. Further experimental studies, such as X-ray profiling, are necessary to clarify the exact location of the metal.

Gold

It is known that unlike chromium or silver, gold coats PS-*b*-PMMA in "nanodrops".[26] As shown in Fig. 3a, these nanodrops are small and dense on PS domains, and larger and sparser on PMMA domains. We believe the difference in sizes and fraction of metal settling on each domain is indicative of the significant difference in both mobility and surface energy of gold-PS and gold-PMMA.[32]

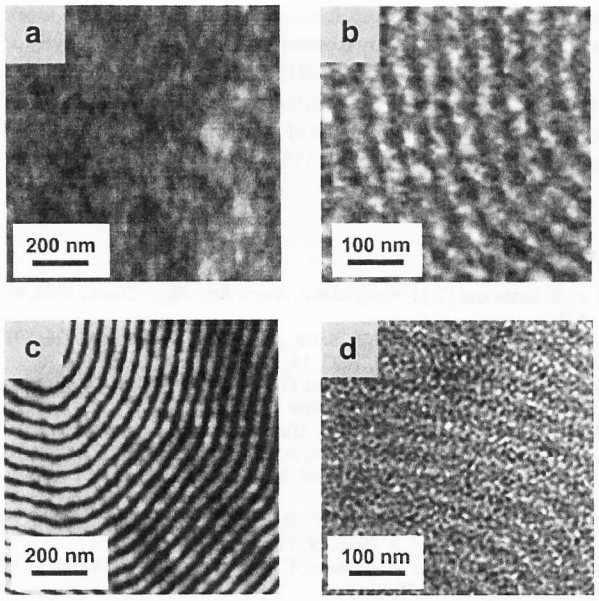

Fig. 2 (a), (c) AFM height and (b), (d) TEM images of PS-*b*-PMMA films coated with 1 nm of chromium, before (a), (b) and after (c), (d) UV exposure, respectively. While the AFM image after UV exposure shows a significant corrugation, showing that PMMA has been removed. The lack of change in TEM images shows that metal lift-off has not occurred, since no clear stripes of metal form.

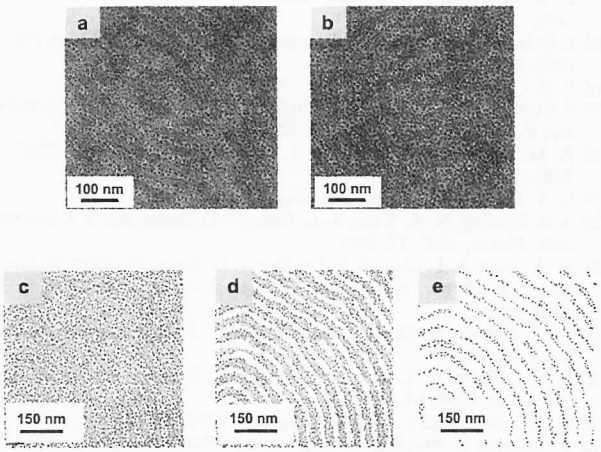

Fig. 3 Au-coated PS-*b*-PMMA films, as seen under TEM. There is little difference between pristine (a) and UV-irradiated (b) samples, suggesting that gold particles remain upon PMMA removal. (c)-(e) A pristine gold-coated PS-*b*-PMMA sample with (c) all of the gold particles, (d) particles on PMMA domains removed by hand, and (e) particles on PS removed.

TEM images provide a two-dimensional projection of a three-dimensional image: the areas of the particles in our images are actually their maximum cross-sectional areas, *i.e.* the projected areas. Applying *Image J* particle counting routines, we can quantify the observed differences of gold on PS and on PMMA. Using a typical 615 × 615 nm^2 image shown in Fig. 3c, we calculated the average maximum cross-sectional area of a gold particle on the diblock overall to be 16.9 ± 8.7 nm^2, and the fraction of total area covered by gold is 26 percent. We then used software to make a copy of the image with gold particles on PMMA removed by hand (Fig. 3d). We could then calculate the gold coverage on PS (40 percent), with the average particle area being 15.6 ± 8.2 nm^2. By using the image subtraction routine we obtained an image with gold only on PS domains, shown in Fig. 3e. We found that the total area of PMMA covered by gold was just 12 percent, with the average particle size of 21.0 ± 9.3 nm^2. For the image we considered, there were about four thousand particles on the PS domains and one thousand on PMMA domains.

We can calculate the ratio of gold volumes which settle on PS and PMMA. If we assume that the particles of gold are drop-like, with the height being equal to the smallest lateral dimension, we can calculate the total volume of gold resting on PS versus PMMA. The total volume for a 615 nm × 615 nm area of diblock for PMMA gold is 72 000 nm^3, and for PS gold is 217 000 nm^3, for a total amount of 281 000 nm^3. The nominal amount of gold deposited was 1 nm × 615 nm × 615 nm ≈ 378 000 nm^3, the same order of magnitude.

The ratio of PS to PMMA gold volume is then approximately 3 to 1 within hours of deposition. PS and PMMA exhibit the same surface area in our films, and gold initially evaporates uniformly everywhere onto the sample, hence at least at first the amount of gold on PS and PMMA should roughly be the same. Therefore, half of the gold from the PMMA diffuses along the surface to PS. This information may be used to design metal–polymer hybrids which would have selective decoration directly after gold deposition, for example by using block copolymers with shorter period spacing, to allow gold to diffuse toward one of the domains.

When we attempted to remove PMMA using UV light by exposing 1 nm Au films on PS-*b*-PMMA, we found there was no change as seen under TEM (Fig. 3b). AFM, however, showed an increase in corrugation from 0.5 nm to 1.5 nm. It is likely that at least some PMMA was removed, causing the increase in corrugation. It is not yet clear whether the relatively low resulting corrugation is the result of an imaging artifact.

Discussion

Nanoscale metal stripes and corrugated surfaces hold promise for a variety of applications, such as electronics, photonics and nanofluidics, as well as creating particle arrays.[20–22,25,33] While it is possible to create such structures using top-down methods, such as e-beam lithography, such methods are extremely time-intensive, as each portion of a pattern is created separately. In this work we have created for the first time a combination of the two types of surfaces: metal-coated surfaces with corrugation on the order of nanometres, using self-assembly. We used diblock copolymer films covered with evaporated metal and irradiated them with UV light.

We know from previous work that UV irradiation has the effect of removing PMMA domains and increasing the sample's corrugation from 0.5 nm to 5 nm.[20,21] Lopes and Jaeger[26] have shown previously that thermal annealing combined with several metal evaporation steps led to the formation of metal nanochains on just one of the two domains of the diblock copolymer films. Initially, we expected UV light to remove part of the metal

together with PMMA, leaving behind only the metal on top of the original PS domains, and forming a corrugated surface covered with metal stripes.

We found that UV exposure did not lead to the formation of metal stripes for films where such stripes were not already present, *i.e.* for gold and chromium on PS-*b*-PMMA. This implies that to create nanochains of gold with nanotroughs separating the chains, for example, one would have to first perform a series of metal evaporation and annealing steps and then the UV exposure. When metal already formed stripes centered on the PS domains, such as in the case of silver, subsequent UV-exposure led to the narrowing of the silver domains, in addition to an increase in corrugation. It is interesting to note that when silver was deposited onto previously-irradiated PS-*b*-PMMA films, there was a faint trace of the underlying fingerprint structure still visible in the TEM images.[34]

The importance of our study is that it brought together for the first time a combination of metal deposition and UV irradiation to create nanoscale structures on diblock copolymer scaffolding. This technique complements other extant methods such as optical or e-beam lithography combined with metal deposition and etching. Our method gives access to creating complex metal/polymer structures on the length scales in the range of 10–20 nm, without requiring creating each individual domain sequentially, as in e-beam lithography.

Conclusions

We have investigated the effects of vacuum UV exposure on three types of metal coatings on diblock copolymer: uniform films, selective nanowires, and partially selective nanodrops. We found that a nanoscale lift-off process does not occur with uniform films. That is, UV light does not create wires out of uniform metal films: while observed corrugation increases under AFM, TEM does not show clear metal stripes. This suggests that metal may still be coating the surface uniformly, although the physical corrugation of the surface is increased. Future studies using conductive AFM will aim to determine whether Cr still remains on the PMMA domains or if the metal dissolved into the polymer. Gold exhibited no change under TEM, while at the same time showing weakly increased corrugation under AFM, suggesting that PMMA was removed without taking any gold with it. This is a surprising finding, since gold does not coat the sample uniformly, and so it should allow most of the PMMA to be removed. In the case of silver, nanowires were narrowed by the use of UV light, which could make them more technologically useful. Previous studies on sequential gold deposition and annealing suggest that combining that technique with UV irradiation should yield a corrugated surface with gold nano-chains.

Acknowledgements

The authors would like to thank Yimei Zheng and Robert Josephs for their assistance with TEM imaging and Daniel Rosenmann for assistance with sputter deposition. We thank Hanqiu Yuan for the lamp intensity measurement. This work was supported by the Army Research Office/DTRA, and by U of C MRSEC grant NSF-DMR-0213745. Use of the Center for Nanoscale Materials was supported by the U.S. Department of Energy, Office of Science, Office of Basic Energy Sciences, under contract No. DE-AC02-06CH11357.

References

1 F. S. Bates and G. H. Fredrickson, *Annu. Rev. Phys. Chem.*, 1990, **41**, 525.
2 G. H. Fredrickson and F. S. Bates, *Annu. Rev. Mater. Sci*, 1996, 501.
3 I. W. Hamley, *Nanotech.*, 2003, **14**, R39.
4 N. Hadjichristidis, S. Pispas and G. A. Floudas, *Block Copolymers*, Wiley Interscience, Hoboken, New Jersey, 2003.
5 M. W. Matsen and F. S. Bates, *Macromolecules*, 1996, **29**, 1091.
6 C. T. Black, R. Ruiz, G. Breyta, J. Y. Cheng, M. E. Coiburn, K. W. Guarini, H.-C. Kim and Y. Zhang, *IBM J. Res. & Dev.*, 2007, **51**, 605.
7 K. W. Guarini, C. T. Black, K. R. Milkove and R. L. Sandstrom, *J. Vac. Sci. Technol. B*, 2001, **19**, 2784.
8 K. Naito, H. Hieda, M. Sakurai, Y. Kamata and K. Asakawa, *IEEE Trans. Mag.*, 2002, **38**, 1949.
9 M. R. Bockstaller, R. A. Mickewicz and E. L. Thomas, *Adv. Mater.*, 2005, **17**, 1331.
10 R. B. Grubbs, *J. Pol. Sci. A*, 2005, **43**, 4323.
11 E. W. Edwards, M. P. Stoykovich, H. H. Solak and P. F. Nealey, *Macromolecules*, 2006, **39**, 3598.
12 J. Y. Cheng, C. A. Ross, V. Z. H. Chan, E. L. Thomas, R. G. H. Lammertink and G. J. Vancso, *Adv. Mater.*, 2001, **13**, 1174.
13 R. A. Segalman, *Mat. Sci. & Eng. R*, 2005, **48**, 191.
14 M. P. Stoykovich, M. Muller, S. O. Kim, H. H. Solak, E. W. Edwards, J. J. de Pablo and P. F. Nealey, *Science*, 2005, **308**, 1442.
15 J. Hahm, W. A. Lopes, H. M. Jaeger and S. J. Sibener, *J. Chem. Phys.*, 1998, **109**, 10111.
16 S. B. Darling, *Prog. Polym. Sci.*, 2007, **32**, 1152.
17 S. O. Kim, H. H. Solak, M. P. Stoykovich, N. J. Ferrier, J. J. de Pablo and P. F. Nealey, *Nature*, 2003, **424**, 411.
18 R. D. Deshmukh, Y. Liu and R. J. Composto, *Nanolett.*, 2007, **7**, 3662.
19 C. T. Black, *IEEE Trans. Nanotech.*, 2004, **3**, 412.
20 S. B. Darling, N. A. Yufa, A. L. Cisse, S. D. Bader and S. J. Sibener, *Adv. Mater.*, 2005, **17**, 2446.
21 N. A. Yufa, A. L. Cisse, S. B. Darling, S. D. Bader, P. Guyot-Sionnest and S. J. Sibener, *Mater. Res. Soc. Symp. Proc.*, 2006, **910E**, 0901-Ra09–06.
22 M. J. Misner, H. Skaff, T. Emrick and T. P. Russell, *Adv. Mater.*, 2003, **15**, 221.
23 R. Z. Zehner, W. Lopes, T. L. Morkved, H. Jaeger and L. R. Sita, *Langmuir*, 1998, **14**, 241.
24 R. Z. Zehner and L. R. Sita, *Langmuir*, 1999, **15**, 6139.
25 N. Kumar, O. Parajuli, A. Gupta and J. Hahm, *Langmuir*, 2008, **24**, 2688.
26 W. A. Lopes and H. M. Jaeger, *Nature*, 2001, **414**, 735.
27 J.-L. Lin, D. Y. Petrovykh, A. Kirakosian, H. Rauscher, F. J. Himpsel and P. A. Dowben, *App. Phys. Lett.*, 2001, **78**, 829.
28 W. A. Lopes, *Phys. Rev. E*, 2002, **65**, 031606.
29 S. B. Darling and A. Hoffman, *J. Vac. Sci. Technol. A*, 2007, **25**, 1048.
30 T. L. Morkved, W. A. Lopes, J. Hahm, S. J. Sibener and H. M. Jaeger, *Polymer*, 1998, **39**, 3871.
31 *Image J* is available free of charge at http://rsbweb.nih.gov/ij/.
32 A. Gopinathan, *Phys. Rev. E*, 2005, **71**, 041601.
33 C. Park, J. Yoon and E. L. Thomas, *Polymer*, 2003, **44**, 6725.
34 N. A. Yufa, S. L. Fronk, S. J. Rosenthal, S. B. Darling, W. Lopes and S. J. Sibener, in preparation.